Research Square

Preprints are preliminary reports that have not undergone peer review.
They should not be considered conclusive, used to inform clinical practice,
or referenced by the media as validated information.

Comprehensive Characterization of Enhanced Performance PLA/TiO2 Packaging Films Synthesized Via Ultrasonication Assisted Solution Casting Process

Anuprita Bhosale
Veermata Jijabai Technological Institute (VJTI)
Dadarao Raut
Veermata Jijabai Technological Institute (VJTI)
Vinod Suryawanshi
vbsuryawanshi@me.vjti.ac.in

Veermata Jijabai Technological Institute (VJTI)
Masidd Khalate
Infinite Biotech Institute of Research and Analytics

Research Article

Keywords: PLA/TiO_2 nanocomposite films, ultrasonication, ethanol pre-treatment, Antibacterial activity, Cytotoxicity, Biodegradable food packing

Posted Date: March 26th, 2026

DOI: https://doi.org/10.21203/rs.3.rs-8645786/v1

License: This work is licensed under a Creative Commons Attribution 4.0 International License.
Read Full License

Additional Declarations: No competing interests reported.

Comprehensive Characterization of Enhanced Performance PLA/TiO_2 Packaging Films Synthesized Via Ultrasonication Assisted Solution Casting Process

Anuprita Bhosale[1], Dadarao Raut[2], Vinod Suryawanshi[3,] Masidd Khalate[4]

[1,2,3]Veermata Jijabai Technological Institute, Mumbai, INDIA

[4]Infinite Biotech Institute of Research and Analytics, Sangli, INDIA

Abstract

This study aims to fabricate poly (lactic acid)/titanium dioxide (PLA/TiO_2) nano composite films for food packaging applications by using ultrasonication-assisted solvent casting approach. Conventional solvent-casting techniques often suffer from TiO_2 particle agglomeration leading to limited functional properties improvements. The proposed method combines ethanol pre-treatment of TiO_2 nanoparticles with prolonged ultrasonication followed by solvent casting. This method ensures uniform nanoparticle dispersion within the PLA matrix. Significant morphological, structural and functional improvements in properties is observed which includes shifts in carbonyl bands indicated in Fourier Transform Infrared Spectroscopy (FTIR), pronounced anatase peaks in X-ray diffraction (XRD). Further, water vapor permeability and water solubility was reduced to 43.5% and 50% respectively. Also, mechanical properties of PLA namely as tensile strength and Young's modulus are increased by 24% and 160%, respectively. Additionally, TiO_2 acts as a strong nucleating agent, enhancing crystallinity and thermal stability, simultaneously hindering the growth of Staphylococcus aureus and Escherichia coli bacteria significantly. Cytotoxicity assessments realised composites' biocompatibility with L929 fibroblast cells.

Overall, this work presents a novel strategy to enhance uniform dispersion of nanoparticles for high-performance, antimicrobial, and thermally stable PLA/TiO_2 nano composite films, paving the way for next-generation biodegradable food packaging solutions.

Keywords: PLA/TiO_2 nanocomposite films, ultrasonication, ethanol pre-treatment, Antibacterial activity, Cytotoxicity, Biodegradable food packing

Introduction

Food packaging becomes a critical element in food preservation and its shelf life. As sustainability becomes a global concern there is a growing demand for biodegradable alternatives that can be a substitute for non-renewable petroleum-based plastics [3,4]. Consequently, polymeric nanocomposites have gained substantial interest as the incorporation of nanoscale fillers can impart a meaningful effect on structural, thermal and barrier properties and enable materials to perform better even under the demanding packaging applications [1,2,5]. Poly (lactic acid) (PLA) remains the best noteworthy renewable source with biodegradability, good transparency and processability [7,8]. However, adoption of PLA in real-life food packaging is hindered due to its poor thermal resistance, average mechanical ability, and inadequate barrier resistance [6,7,14,42].

Titanium dioxide (TiO_2) NPs offer distinct advantages which can markedly improve barrier thermal, and mechanical properties of PLA, while simultaneously enhancing the antibacterial activity which is an essential element for the packaged food in terms of shelf life [43]. However, producing high performance PLA/TiO_2 nanocomposite films remains challenging as uniform dispersion of TiO_2 nanoparticles in polymer matrix is difficult. Conventional solution-casting method do not effectively address this problem, often leading to inconsistent property enhancement. [2,11,20,35].

To address this challenge, the current work employs a convenient and efficient solution, consisting of pre-wetting of TiO_2 nanoparticles (NPs) in ethanol followed by ultrasonication throughout the film formation. Ultrasonication is described to deform the clusters of NPs by acoustic cavitation, but its application in the formation of PLA/TiO_2 films has not been examined in detail [12,18,31].

This study focuses on developing PLA/TiO_2 nanocomposite films with 1%, 3% and 5 wt% TiO_2 using ultrasonication-aided solvent-casting technique, and evaluate their thermal, mechanical, morphological, barrier, antibacterial and cytocompatibility properties.

Materials and Methods

Materials

The base materials consist of polylactic acid (PLA) having melt flow rate of 7 g/10 min purchased from Solidspace Technology, Nashik, India and titanium dioxide nanoparticles (TiO_2-NPs) of 99.5% purity with an average particle size of 10-30 nm were purchased from Platonic Nanotech, Jharkhand, India. Chloroform of 99.5 % purity solvent was used to dissolve PLA and disperse the nanoparticles.

In the case of antimicrobial analysis, the *Staphylococcus aureus* (Gram-positive) and *Escherichia coli* (Gram-negative) strains were utilized. Cytotoxicity of samples was evaluated using L929 mouse fibroblast cells.

Composition and designation of PLA and PLA/TiO_2 Nanocomposite Films

PLA and PLA/TiO_2 nanocomposite films were prepared using ultrasonication assisted solvent-casting technique. TiO_2 nanoparticles were incorporated at different loadings of 1%, 3% and 5% (w/w relation to PLA). These produced films were labelled as PT-01, PT-03 and PT-05 respectively, corresponding to the TiO_2 loadings.

Methods

Preparation of PLA Films

The PLA granules were first dried in a hot air oven set at 50 °C for 24 hours in order to remove moisture. To prepare the film, two grams of PLA was dissolved in 20 mL of chloroform, and the mixture was continuously stirred with the help of a magnetic stirrer at room temperature (27 °C) until a clear, uniform solution is created.

The PLA solution was then applied on glass plate to produce a film with uniform thickness of 120 µm by using a bird type film applicator. The casted film was left at room temperature for 24 hours to evaporate the solvent. The dried films were kept in hot air oven at 60 °C for 4 hours to eliminate residual chloroform. Following careful removal from the glass plate, the films were allowed to cool to ambient temperature before being placed in sealed containers for further analysis.

Preparation of PLA/TiO_2 Nanocomposite Films

To prepare nanocomposites, the required amount of TiO_2 nanoparticle was first weighed and surface treated using ethanol in order to enhance their dispersion. TiO_2 nanoparticles are highly surface-energetic, and therefore, they are prone to agglomerate which limits their compatibility with organic solvents and polymer matrices unless they are pre-treated [5]. Ethanol was used as a short-term dispersing agent, which facilitated good wetting and partial deagglomeration of the nanoparticles.

After evaporation of the ethanol, TiO_2 nanoparticles were re-dispersed in chloroform and ultrasonicated at room temperature to allow a stable suspension to form. The TiO_2 suspension was then gradually added to the already prepared PLA solution and the mixture continuously was stirred for an hour to promote uniform dispersion of TiO_2 nanoparticles in polymer matrix.

Finally, the PLA/TiO_2 nanocomposite solution was deposited on the clean glass plates (15 cm x 20 cm) and casted evenly with a bird eye type film applicator.

After 24 hours of drying period at ambient temperature, the films were subjected to 4-hour heat treatment at 60 °C to remove any residual solvent. The nanocomposite films were then gently peeled off and stored under ambient conditions for subsequent characterization.

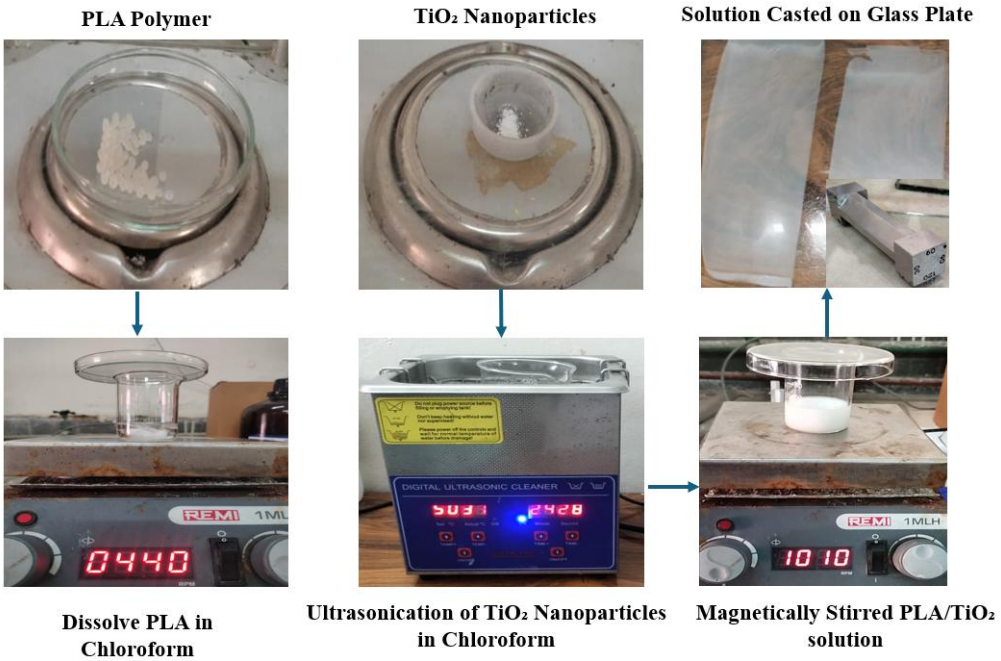


Figure_1 Preparation of PLA/TiO_2 nanocomposite films

Characterization

Fourier Transform Infrared Spectroscopy (FTIR)

ATR-FTIR study was accomplished using a Nicolet Summit X spectrometer (Thermo Fisher Scientific, USA) equipped with an Everest ATR accessory (Smart Accessory ID: B122111) and a DTGS KBr detector. The instrument was operated with a KBr beam splitter and a sample spacing of 1.0 cm^{-1}. For each sample, 16 scans were collected at a resolution of 4 cm^{-1} and around, 16 background scans were recorded under the same conditions. The aperture was maintained at 100%, and the optical velocity was set to 0.4747 cm/s. Spectral data was collected over the range of 4000–400 cm^{-1}. Prior to interpretation, all spectra were baseline corrected to ensure accurate comparison between the samples [5,20].

X-Ray Diffraction

To perform X-ray diffraction (XRD) analysis, an EMPYREAN diffractometer with a Cu Kα radiation source (λ = 1.5406 Å) running at 45 kV and 40 mA was used. To assess the crystalline structure of PLA and PLA/TiO_2 nanocomposite film, diffraction patterns were collected over a 2θ range of 5° to 70°. With the help of obtained data, changes in the diffraction peaks due to TiO_2 presence and its crystallinity were evaluated [21,22].

Scanning Electron Microscopy

High-resolution scanning electron microscope (SEM; JSM-IT800) at an accelerating voltage of 5 kV was employed to evaluate surface morphology of the films. Films were cut into small pieces of about 1 x 1 cm^2 and attached on clean metal stubs. A thin layer of gold (5-10 nm) sputter-coated on each of samples under vacuum conditions to enhance the conductivity of the surface and get better images. The coated films were subsequently analyzed using SEM and the microstructural characteristics were recorded to compare them with various formulations [23].

Mechanical Characterization

Tensile Testing

A universal testing machine with a 5 kN load cell and a crosshead rate of 10 mm 10 min^{-1} was used to evaluate the tensile performance of the films according to ASTM D882-10 [49]. The films were cut into rectangular shapes with dimensions of 2.5cm x 10 cm to maintain sample uniformity. All strips were meticulously clamped into the machine grips to make sure that they were aligned properly so that they did not slip or cause uneven stress distribution during the testing process. The tensile strength (σ_t) and elongation at break (ε) of each sample were recorded by the instrument software. Mean values of the five independent replicates were computed for each type of film to achieve reliability and reproducibility of the measurements [24].

Thermal Characterization

Thermal behaviour of films was analyzed by thermogravimetric analysis (TGA) and differential scanning calorimetry (DSC) using an instrument called a DSC Q2000 (V24.11 Build 124).

The DSC thermal cycle consisted of:

I. Heating from 40 °C to 200 °C at 100 °C·min^{-1},
II. Isothermal holding at 200 °C for 5 min,

III. Cooling from 200 °C to 10 °C at 20 °C·min^{-1},
IV. 5 min isothermal hold at 10 °C, and
V. Second heating from 10 °C to 200 °C at 20 °C·min^{-1}.

The glass transition temperature (T_g), cold crystallization temperature (T_{cc}), and melting temperature (T_m) were obtained from the second heating and cooling scans to ensure reproducible thermal property evaluation [25].

Thermogravimetric analysis was carried out at the temperature of 30 °C to 750 °C at 10 °C /min with a nitrogen atmosphere. Thermograms were assessed to determine residual mass, maximum degradation temperature (T_{max}), and onset degradation temperature (T_{onset}), which reflected how addition of TiO_2 NPs influence thermal stability of PLA films.

Water Solubility

Water solubility of the films was demonstrated by following the method described in [11]. The film samples were prepared by cutting them into 2cm x 2cm squares and drying them at 105 °C for 24 hours in a hot-air oven to remove moisture. Each specimen was dried and the initial dry weight (W_i) was measured. 50 mL of distilled water was added to the samples, followed by a 24-hour gentle stirring to dissolve the water-soluble components. The solution was then filtered through Whatman No. 1 filter paper to collect the undissolved residues. The rest of the solids were dried for 24 hours at 105 °C then the final dry weight (W_f) was obtained.

The degree of water solubility (%) was determined using:

$$\text{Solubility (\%)} = \frac{W_i - W_f}{W_i} \times 100$$

This parameter indicates the concentration of the film dissolved in water and gives an idea about the solubility, and applicability of the PLA based materials in the packaging [26].

Water vapor permeability measurement

According to ASTM E96-2005 [47], the water vapor permeability of PLA and PLA/TiO_2 film was assessed. The experiments were conducted at 25 °C and 50% relative humidity (RH).

The film samples were firmly sealed around the mouths of the pre-weighed test cups that contained a desiccant and only the exposed surface of the film could transmit moisture. The cups were then put in a humidity-controlled chamber and the mass gain was measured at intervals as the water vapor permeated through the films.

Values of water vapor transfer rate (WVTR) were obtained directly from the instrument; the water vapor permeability (WVP) was estimated using the following equation:

$$WVP = \frac{WVTR \cdot L}{\Delta P}$$

Where:

WVTR = water vapor transfer rate (gm^{-2} day^{-1}) as determined by the mass gain.
L = film thickness (m)

ΔP = difference between the vapor pressure on one surface of the film (Pa) and one on opposite surface (Pa).

Each sample was analysed in triplicates and mean WVP values were calculated.

Antibacterial Testing

The antibacterial performance of PLA and PLA/TiO_2 composite film was assessed using the agar well diffusion assay on nutrient agar plates. Sterile petri dishes were filled with nutrient agar was left to dry. Bacterial culture (0.1 mL) of each test strain was uniformly spread on the agar surface using sterile cotton swab to ensure even inoculation.

Film samples of the same size were carefully inserted into wells that were aseptically punched into the solidified agar. The diameter of each well was about 0.6 cm. The plates were then incubated for 24 hours at 37 °C. After the incubation period the diameter of the clear inhibition zones developed around the wells was measured to obtain the antibacterial performance. Inhibition zones for both Gram-positive *Staphylococcus aureus* and the Gram-negative *Escherichia coli* were measured in millimeters [28,29].

Cytotoxicity Assessment (MTT Assay)

The MTT colorimetric test assesses cellular metabolic activity as an indicator of cell viability in accordance with ISO 10993-5:2009. This assay was used to determine the cytotoxicity of neat PLA and PLA/TiO_2 nanocomposite films [48]. L929 mouse fibroblast cells were used as the model cell line, and 5-fluorouracil was included as the positive (cytotoxic) control.

In 96-well plates, cells were seeded at a density of 1×10^2 cells/well and were left to adhere for 24 hours at 37°C with 5% CO_2. After that, film-treated media was used for cell treatment. Untreated cells were served as the negative control. Blank cells containing only medium was used for background corrections. After 24 hours of exposure, 10–20 µL of MTT reagent (5 mg/mL) was added to each well, and the wells were incubated for three to four hours until

purple formazan crystals formed. After carefully removing the medium, 100 µL of DMSO was added to dissolve the crystals.

A microplate reader was used to measure the absorbance at 570 nm, with 630–690 nm serving as the reference wavelength wherever necessary. The ratio of cell practicality was determined in comparison to untreated controller cell using:

$$\text{Cell viability (\%)} = \frac{\text{OD}_{\text{sample}}}{\text{OD}_{\text{control}}} \times 100$$

Percent inhibition was determined, as:

"Inhibition (%)"=100-"Cell viability (%)"

All experiments were performed three times, and mean results are reported.

Results and Discussion

Fourier Transform Infrared Spectroscopy (FTIR)

The FTIR spectra of neat PLA and PLA/TiO_2 nanocomposite films (PT-01, PT-03, PT-05) presented in figure 2 indicate the interaction among the nanoparticles and polymer matrix. The figure shows that all samples have the typical PLA characteristics, a robust ester carbonyl band at 1745 cm^{-1} [19, 37], C-H stretching bands in the 3000-2800 cm^{-1} range [37], methyl bending vibrations at 1450 and 1380 cm^{-1} [37], and C-O-C/C-O bands in 1300-1000 cm^{-1} region [17].

On the addition of TiO_2, the carbonyl peak changes slightly to lower wavenumbers and becomes broader (Figure 2) indicating that the ester groups interact with TiO_2 nanoparticles, probably through hydrogen bonding or coordination with surface Ti^{4+} ions [5,9]. The O-H stretching region [3200-3600 cm^{-1}] is increased and intensified with increased hydrogen-bonding network in the interface [14,17]. Additional evidence of the presence of TiO_2 and its interaction with the polymer backbone is the subtle alteration of the 1200-1000 cm^{-1} region and the emergence of new peaks in the 800-400 cm^{-1} range [11,9].

Overall, according to figure 2, TiO_2 nanoparticles are not passive fillers, but are able to interact with PLA chains, which actively contribute towards better crystallinity, mechanical reinforcement and thermal stability of films [5,14].

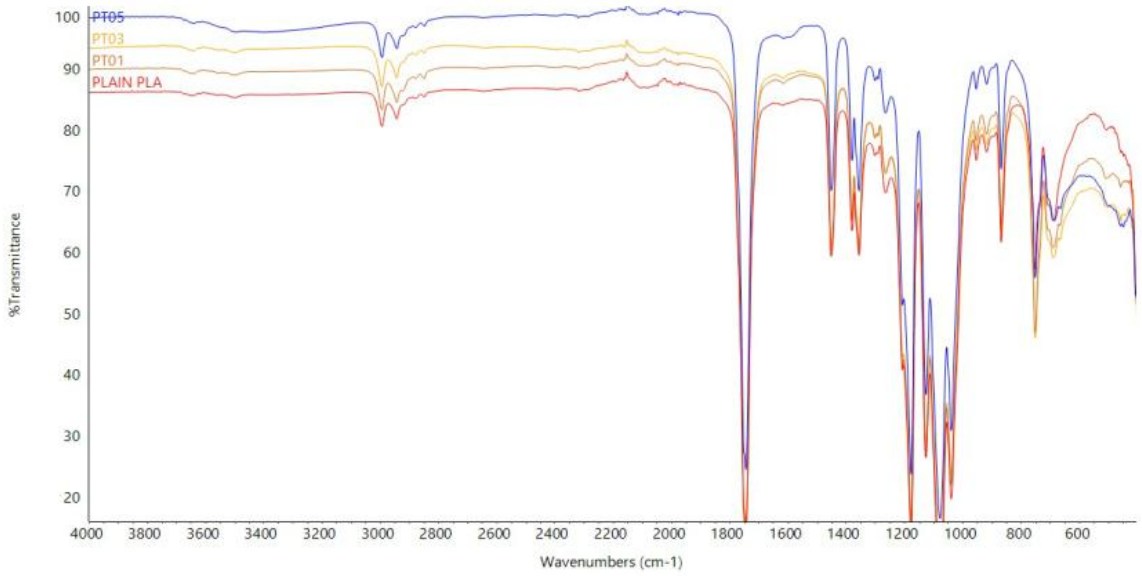


Figure_2 FTIR spectra of neat PLA and PLA/TiO_2 composite films

X-Ray Diffraction

XRD patterns (Figure 3) of neat PLA and PLA/TiO_2 nanocomposite films (PT-01, PT-03, PT-05) are illustrating the structural changes induced by nanoparticle incorporation. The neat PLA film exhibits broad diffraction peaks around 16.7° and 19°, which is the indication of its semicrystalline nature with relatively low crystallinity [37,40].

Upon adding TiO_2, new diffraction peaks appear at approximately 25°, 37°, and 48°, corresponding to the (101), (004), and (200) planes of anatase TiO_2, confirming the successful incorporation of nanoparticles within the polymer matrix [5,11,14]. With increasing TiO_2 content, peak intensities gradually increase and full width at half maximum (FWHM) values narrow, indicating enhanced crystallinity due to the nucleating effect of TiO_2, which facilitates more ordered polymer chain alignment [40,41].

Among the composites, PT-03 shows a balanced combination of nanoparticle dispersion and crystallinity, whereas PT-05 exhibits sharper TiO_2 reflections, suggesting partial agglomeration at higher loadings. Overall, the XRD results confirm strong interfacial interactions between PLA and TiO_2, improved structural organization, and successful nanocomposite formation, which are expected to enhance barrier and thermal properties of the films [5,14,40].

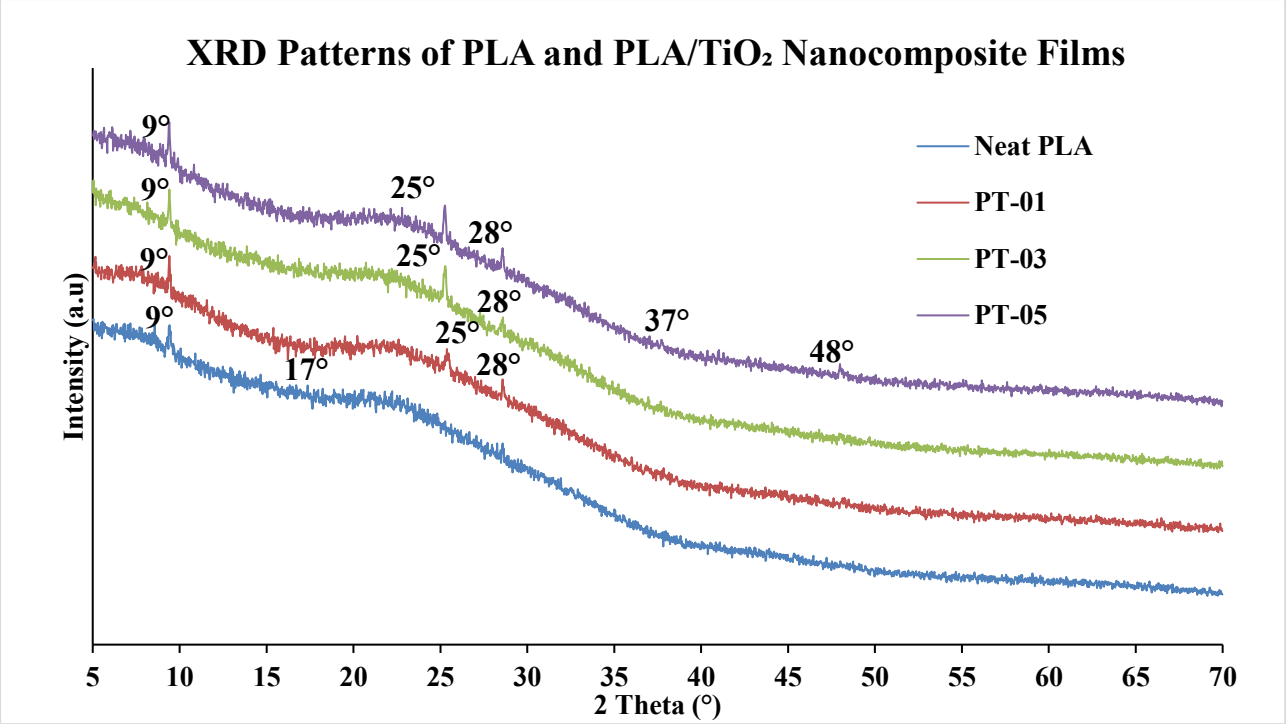


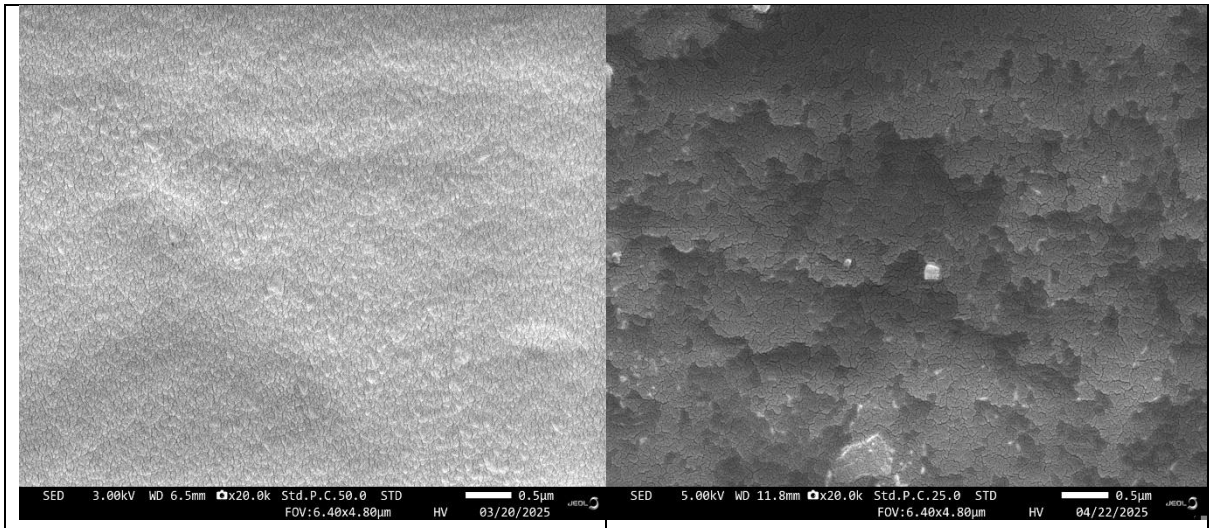
Figure 3 X-ray diffraction (XRD) graphs of pure PLA and PLA/ TiO_2 nanocomposite films:

Scanning Electron Microscopy (SEM) Analysis

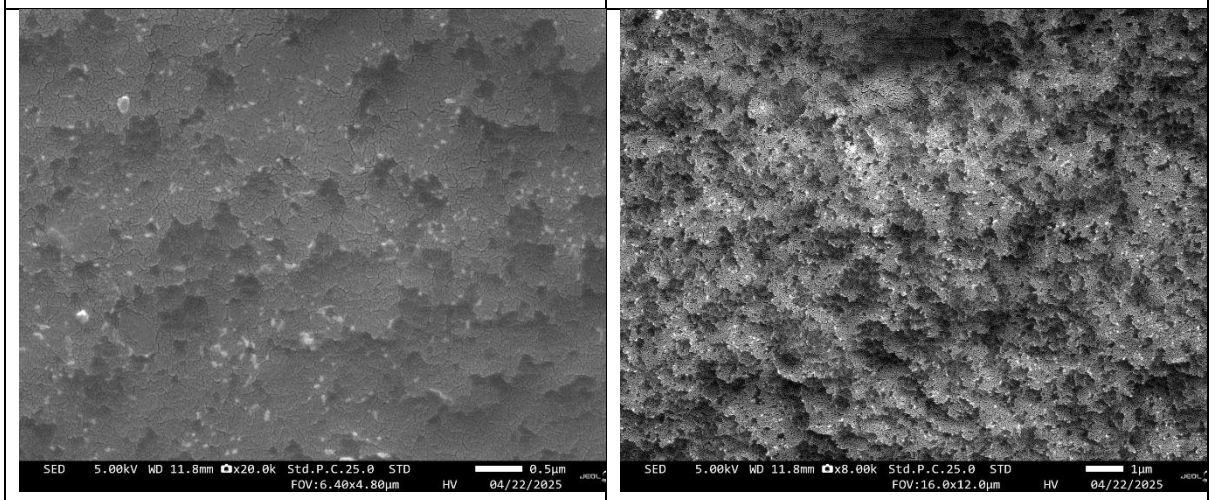
Figure 4 represents SEM micrographs of neat PLA and PLA/TiO_2 nanocomposites films. The neat PLA (Figure 4a) has a smooth and homogenous surface which is indication of brittle properties and no reinforcing filler [37,40].

However, at 1% TiO_2 (PT-01, Figure 4b), the surface is a little coarser and the nanoparticles are well dispersed with minimal agglomeration, which means the adhesion with the interface occurs fairly well and that stress transfer occurs effectively [11,14]. The 3 wt.% sample (PT-03, Figure 4c) exhibits predominantly uniform dispersion with isolated TiO_2 agglomerates, indicating partial aggregation that may contribute to increased stiffness but could also introduce localized stress concentration sites [5,40]. The structure becomes strongly agglomerated at 5 wt% (PT-05, Figure 4d), demonstrating irregular surface morphology interfering the continuity of the matrix, leading to poor mechanical performance [5,14].

These morphological findings are consistent with trends in mechanical and thermal properties, indicating that nanoparticle dispersion and interfacial adhesion are important in the performance enhancement of PLA/TiO_2 nanocomposites when used in food packaging.



a. NEAT PLA **b.** PT-01



c. PT-03 **d.** PT-05

Figure_4 Scanning Electron Microscopy (SEM) analysis of neat PLA and PT composites TiO_2.

Tensile Properties of PLA/TiO_2 Nanocomposites

The tensile characteristics of PLA and PLA/TiO_2 nanocomposite films were examined in order to compare the reinforcing effect of TiO_2 nanoparticles. Figure 5 indicates a bar chart of all samples summarizing tensile strengths (σ_t) and elongation at break (ε).

Figure 5 demonstrates that neat PLA has a typical brittle stress strain response with σ_t equal to 60.0 MPa and ε equal to 4.19% [37,40]. TiO_2 incorporation enhances the mechanical performance: σ_t is 63.8 MPa (PT-01) and 74.6 MPa (for both PT-03 and PT-05) which is increased by almost 24%. The Young's modulus is also significantly increased compared to

1,432.7 MPa of neat PLA to 2,149.2 MPa, 3,243.5 MPa, and 3,730.0 MPa of PT-01, PT-03, and PT-05, respectively, with an increase of about 50, 126 and 160 %, respectively [5,14,40].

The increase in tensile strength (σ_t) and stiffness is primarily related to the uniform dispersion of TiO_2 nanoparticles and improved adhesion at the polymer–filler interface, allowing more efficient stress transfer within the composite structure. The nanoparticles inhibit chain mobility and serve as centres of loads, which increase elastic resistance. The σ_t plateau at loads above 3 wt.% indicates that slight agglomeration at higher loadings may prevent additional strength enhancement although the stiffness continues to increase [11,14].

In contrast, ε decreases gradually with increasing TiO_2 loading, 4.19% for neat PLA to 2.97%, 2.30%, and 2.00% in PT-01, PT-03, and PT-05, respectively (Figure 4). This ductile decrement is due to the fact that TiO_2 particles are stress concentrators that inhibit plastic deformation. Such trade-off between increased stiffness and decreased flexibility is commonly observed in nanoparticle-reinforced polymers [5,40].

Among the formulations, PT-03 (3 wt.% TiO_2) demonstrates the most optimal balance of mechanical properties, combining elevated tensile strength (σ_t) and stiffness with a moderate elongation (ε). Altogether, the current findings affirm that TiO_2 nanoparticles are effectively incorporated into PLA matrix leading to enhanced tensile properties by having a good matrix-filler interaction and controlled dispersion [5,11,14].

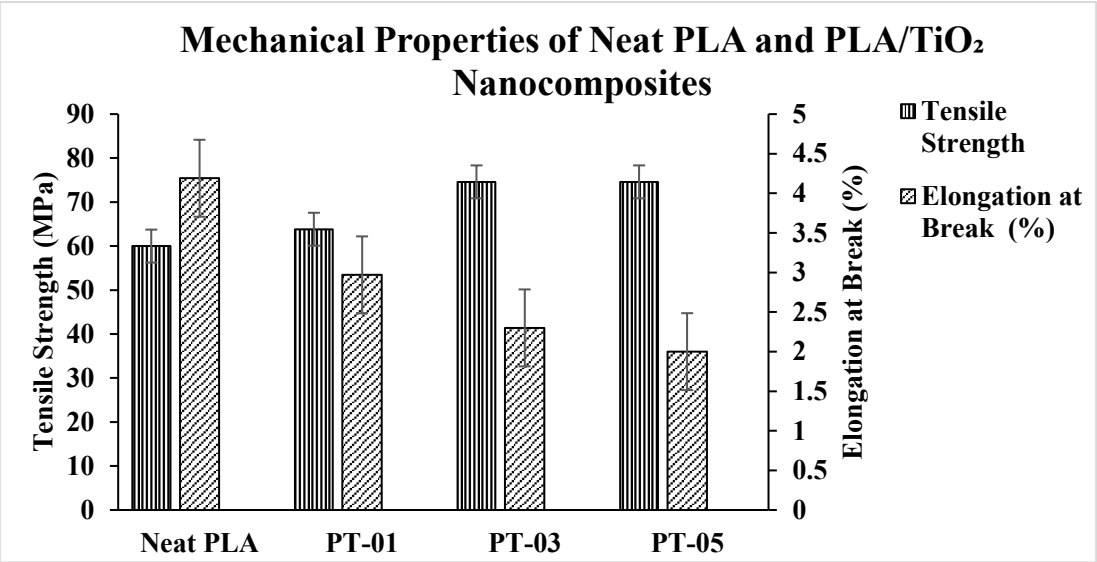


Figure 5 Tensile characteristics of neat PLA and PLA/TiO_2 nanocomposites (σ_t: tensile strength, ε: elongation at break). Data is a mean of five independent samples, which indicates the influence of TiO_2 loading on mechanical performance.

Water Vapor Permeability (WVP) of PLA and PLA/TiO_2 Nanocomposites

Neat PLA and PLA/TiO_2 nanocomposite films were assessed to determine performance of the water vapor barrier through ASTM E96 desiccant method at 25 °C and 50% relative humidity (RH) [27, 47]. To calculate the WVP values, the following method was used:

$$\text{WVP} = \frac{\text{WVTR} \times L}{\Delta P}$$

L: the thickness of the film (≈120 μm) and ΔP: the change in partial pressures of water vapour across the film. The findings can be summarized in Table 1 and represented in Figure 6.

WVP of neat PLA is 16.44 g mm m^{-2} day^{-1} kPa^{-1} as illustrated in figure 6. Integration of TiO_2 nanoparticles resulted in significant decrease in WVP and enhanced barrier properties. At 1 wt% TiO_2 (PT-01), WVP reduced by 18.3%, which means that nanoparticles can disrupt vapor transmission causing the diffusion pathway to become more tortuous. The reduction was attenuated at 3 wt % (PT-03) with a 35.8 % decrease, indicating optimum dispersion contributes to formation of more effective tortuous diffusion pathway the PLA matrix [34]. At 5 wt% (PT-05), WVP declined slightly to 9.30 g mm m^{-2} day^{-1} kPa^{-1} (-43.5%), as at higher concentrations due to nanoparticle agglomeration

The trends of WVP observed in this research are in agreement with the literature where the PLA/TiO_2 nanocomposite films showed reduced WVP by 30-45% at 3-5 wt% TiO_2 loading [32-33].

Overall, the results demonstrate that incorporation of TiO_2 nanoparticles can improve water vapor permeability of PLA films', with 3 wt% providing the balance between the barrier effect and the nanoparticle's dispersion.

Table 1. Water Vapor Permeability (WVP) of PLA and PLA/TiO_2 Nanocomposite films.

Sample	WVTR ($g\ m^{-2}\ day^{-1}$)	WVTR ($mg\ cm^{-2}\ hr^{-1}$)	WVP ($g\ mm\ m^{-2}\ day^{-1}\ kPa^{-1}$)	% Reduction
Neat PLA	192.4	0.802	16.44	–
PT-01	157.3	0.655	13.44	18.3%
PT-03	123.6	0.515	10.56	35.8%
PT-05	108.9	0.454	9.30	43.5%

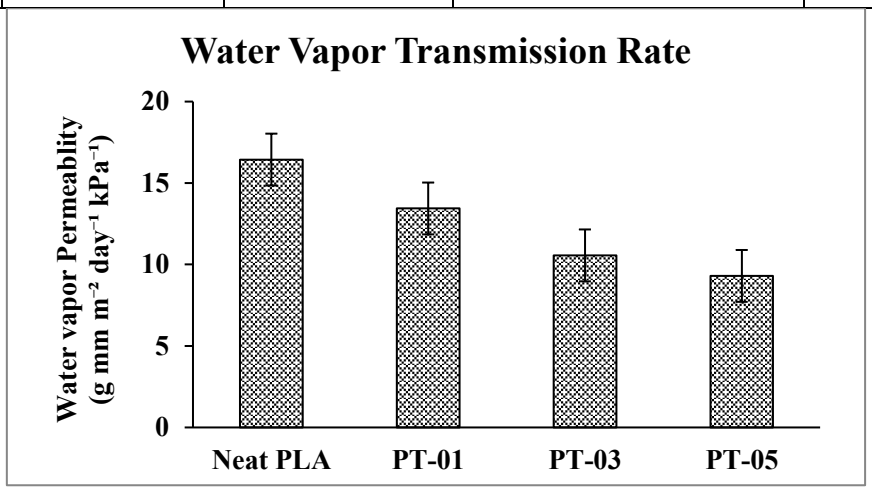


Figure_6 Change in water vapor permeability (WVP) of the neat PLA and PLA/ TiO_2 nanocomposites films with the adding of TiO_2.

Water Solubility

Figure 7 shows the water solubility (WS) of neat PLA film and PLA/TiO_2 nanocomposite films. Neat PLA had a solubility of around 10 %, indicating that PLA is moderately hydrophobic and interacts minimally with water molecules [37,40].

Addition of TiO_2 nanoparticles gradually reduced WS as the concentration of nanoparticles increased. When TiO_2 (PT-01) concentration was increased to 1 wt%, WS decreased

remarkably to about 8% suggesting that early development of a denser polymer matrix inhibits the penetrability of water. At 3 wt% loading a significant reduction approximately 6% was recorded. This behaviour is associated with improved nanoparticle dispersion, leading to better interfacial adhesion and longer tortuous path for mater molecules. At a TiO_2 content of 5 wt.% (PT-05), water solubility dropped to around 5%, but the improvement became less pronounced, possibly as a result of nanoparticle agglomeration at elevated concentrations [35,36]. The gradual decrease in WS shows that TiO_2 NPs increase hydrophobic nature and water resistance of PLA films. This reduction results from the development of tortuous diffusion paths due to uniformly dispersed nanoparticles, which restrict molecular diffusion, along with the nucleating effect of TiO_2 that enhances crystallinity and limits the free volume accessible to water uptake [35,36].

In summary, the findings indicate that the incorporation of TiO_2 nanoparticles effectively enhances the water-resistant behavior of PLA, supporting its potential use in biodegradable food packaging materials.

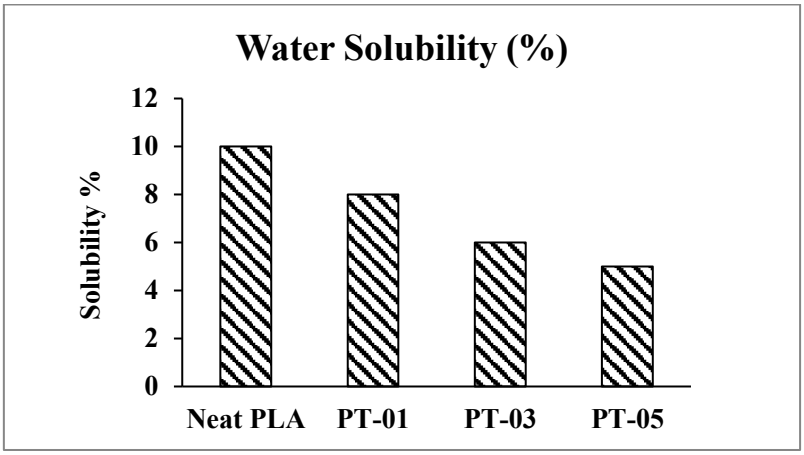


Figure_7 Neat PLA and PLA/TiO_2 nanocomposite film water solubility (%)

Thermogravimetric Analysis (TGA)

The thermal properties of neat PLA and PLA/TiO_2 nanocomposites were investigated by TGA and DSC in order to evaluate the effect of TiO_2 nanoparticles on polymer stability and crystallization characteristics. TGA curve (Figure 8) and DTG profiles (Figure 9) indicate that neat PLA decomposes in a single step initiating at approximately 320 °C and peaks at approximately 360-365 °C, as a characteristic of aliphatic polyesters [37].

The degradation behaviour was influenced by addition of TiO_2 nanoparticles resulting in higher residual mass at higher temperatures. Neat PLA revealed a residual mass of around 4.3% at 400 °C, whereas PT-01, PT-03, and PT-05 retained approximately 8.1%, 5.8%, and 8.0% of their original mass at the same temperature. This is because of the thermally stable TiO_2 particles which serve as a heat resistant and retard the release of volatile degradation products [38-39].

These observations can also be confirmed by DSC study (Table 3). The glass transition temperature (T_g) was almost same (approximately 54.7-54.8 °C) indicating that the nanoparticles do not considerably limit the mobility of the amorphous polymer chains. Nevertheless, crystallization temperature (T_{cc}) and degree of crystallinity (χ_c) were influenced by the addition of TiO_2. The T_{cc} of neat PLA was 78.4 °C with low crystallinity ($\chi_c \approx 1.97\%$). When TiO_2 was added T_{cc} decreased and crystallinity increased, which means that the nanoparticles act as nucleation sites and promote polymer chain ordering. PT-01 and PT-05 exhibited T_{cc} values of 70.6 °C and 71.5 °C, along with χ_c values of 3.23% and 3.79 %, respectively, whereas PT-03 exhibited intermediate values ($T_{cc} \approx 78.9$ °C; $\chi_c \approx 2.29\%$) probably due to partial nanoparticle aggregation [40].

The melting temperature of the PLA/TiO_2 nanocomposites was 167–169 °C, higher than that of neat PLA (148.8 °C), and is in agreement with the typical PLA crystallization behaviour. The observed rises in enthalpy of melting (ΔH_m) and χ_c of PT-01 and PT-05 represent an enhanced crystalline structure, and no higher-temperature shoulders detected due to secondary melting or recrystallization [41-42].

In general, TGA and DSC data indicate that TiO_2 NPs can enhance thermal properties of PLA in two aspects: (i) by offering a thermally stable barrier to increase the amount of char and delay decomposition, and (ii) by serving as nucleation sites to promote crystallinity and alter crystal structure. The said effects are mostly evident in PT-01 and PT-05, whereas PT-03 exhibits moderate increase because the particles are not dispersed much. Notably, it can be stated that all the samples are thermally stable to approximately 300 °C and this suggests that incorporation of TiO_2 does not compromise intrinsic thermal characteristics of PLA which is encouraging in terms of packaging and other applications that require high heat stability.

Table 3. DSC parameters of neat PLA and PLA/TiO_2 nanocomposite films

Sample	T_g (°C)	T_{cc} (°C)	T_m (°C)	ΔH_m (Jg^{-1})	χ_c (%)
PLA (neat)	54.7	78.4	148.8	1.083	1.97
PT-01 (1 wt% TiO_2)	54.8	70.6	167.2	1.363	3.23
PT-03 (3 wt% TiO_2)	54.8	78.9	168.1	0.833	2.29
PT-05 (5 wt% TiO_2)	54.7	71.5	167.5	1.482	3.79

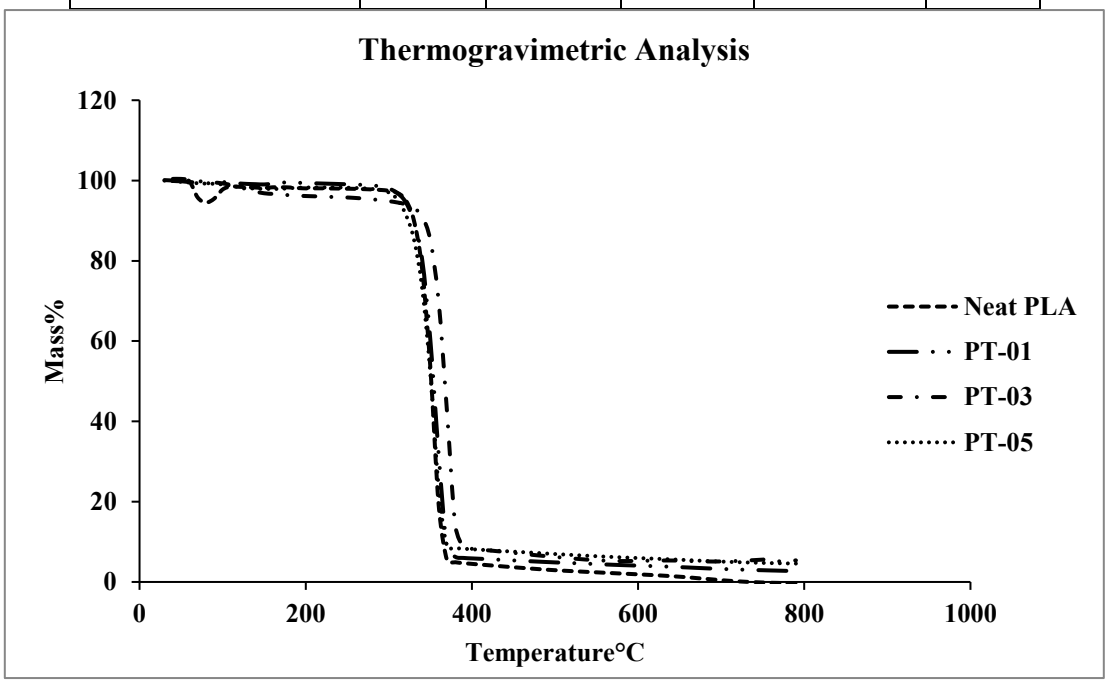


Figure_8 Thermogravimetric Analysis (TGA) of Neat PLA and PT Composites

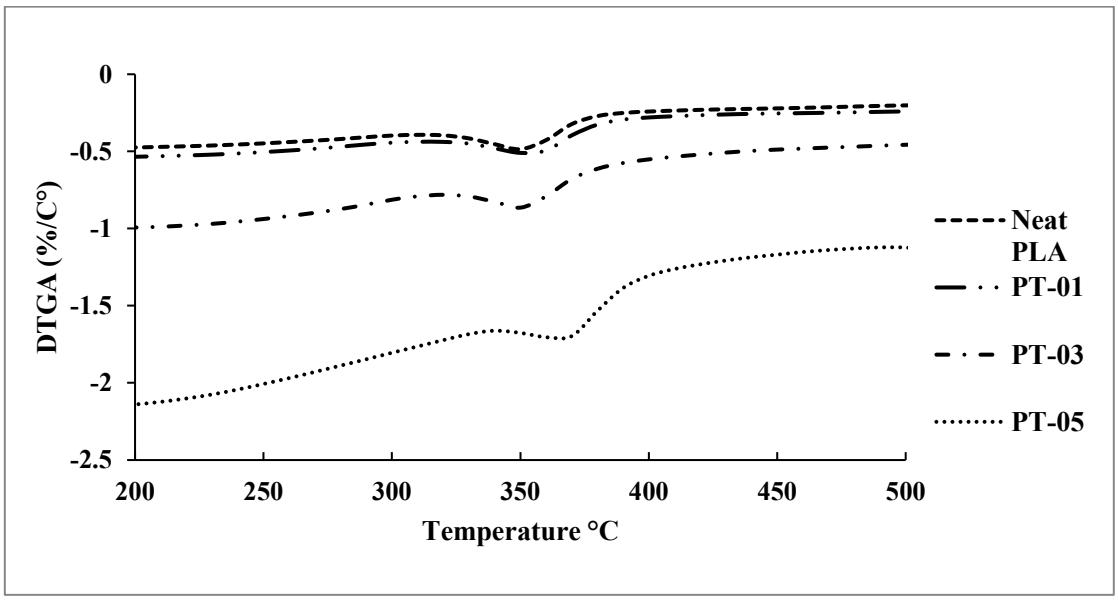


Figure_9 Derivative thermogravimetric (DTG) curves of neat PLA and PLA/TiO_2 nanocomposite films, which indicates the decomposition rate and thermal stability change with varying TiO_2 loading.

Antibacterial Activity

Using the agar well diffusion technique, the antibacterial activity of the neat PLA and PLA/TiO_2 nanocomposite film was assessed against gram-positive *Staphylococcus aureus* and gram-negative *Escherichia coli* bacteria (Figures 10 and 11). Neat PLA had no inhibition zones as anticipated because it lacked an intrinsic antibacterial effect.

Integrating TiO_2 nanoparticles greatly enhanced the antibacterial performance, and the inhibition zones increased with higher TiO_2 content. The 1 wt% of TiO_2 (PT-01) showed moderate antibacterial activity with the inhibition zone of 16 mm for both E. coli and S. aureus. More addition of TiO_2 up to 3 wt% (PT-03) improved the activity with an inhibition zone of 18mm (E. coli) and 21mm (S. aureus). The highest activity was found for PT-05 (5 wt% TiO_2) with inhibition zone of 22 mm and 23 mm, respectively.

As reported in literature [1], the antimicrobial activity is greater against S. aureus as compared to E. coli, probably because of cell wall construction variations. Gram positive bacteria have thicker and more peptidoglycan layer which facilitates easier interaction with TiO_2 nanoparticles. In contrast, Gram negative bacteria possess an outer layer of lipopolysaccharide that limits nanoparticle penetration.

The increased antibacterial activity with increased TiO_2 loading may be explained by the following reasons: (i) more surface area of TiO_2 nanoparticles to produce reactive oxygen species (ROS) in presence of light, (ii) increased contact between nanoparticles and bacterial cells, and (iii) increased exposure of nanoparticles at the surface of the film. Interestingly, the improvement between PT-03 and PT-05 indicates that 3 wt.% TiO_2 could be an optimal dispersion level as nanoparticle agglomeration at higher concentrations slightly reduce efficiency gains [43-44].

Similar concentration-dependent antibacterial behaviour has been reported for PLA/TiO_2 nanocomposites in earlier studies by [45,46]. It can be concluded that the addition of TiO_2 is a truly efficient method of giving PLA films antibacterial activity and thus suitable for active packaging.

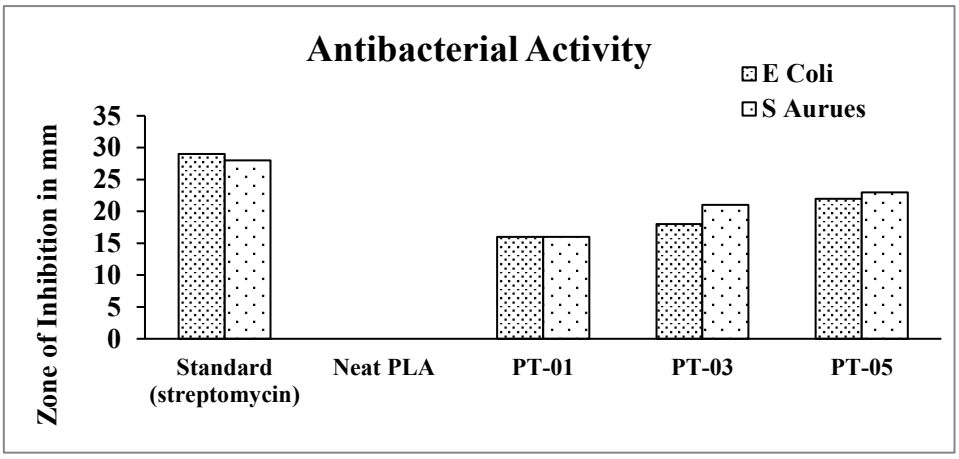


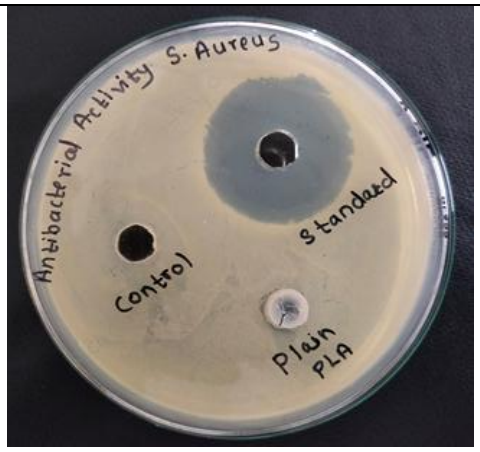
Figure_10 Neat PLA and PLA/TiO_2 nanocomposite films Agar well diffusion method of evaluating antibacterial action against E. coli and S. aureus



E Coli PLA



E Coli PT



PLA-S Aureus



S Aureus PT

Figure_11 The photograph of the agar well diffusion process of the antibacterial movement of neat PLA and PLA/TiO_2 nanocomposites films on E. coli and S. aureus agar plate, where the agar plate shows the size of the agar wells.

Cytotoxicity Study

The cytocompatibility of clean PLA and PLA/TiO_2 nanocomposite films (PT-01, PT-03, and PT-05) was assessed using an in vitro cell culture assay to measure their eligibility for safe usage in packaging and biomedical applications. The vehicle control recorded an absorbance of 1.482. PLA and its nanocomposite film recorded an absorbance of 1.256, 1.242, 1.225, and 1.196 for neat PLA, PT-01, PT-03, and PT-05, respectively which were slightly less than absorbance of control. The inhibition values were relatively low, measuring 15.2% for neat PLA and 19.3% for PT-05, suggesting that none of the samples showed significant cytotoxicity under ISO 10993-5 guidelines [48].

These results were further confirmed by microscopic analysis of treated cells (Figure 13). Cells showed normal morphology, confluence and attachment in all formulations without any apparent detachment, rounded or lysed cells. Even at the highest TiO_2 loading (5 wt%), PT-05 did not produce negative impact on cell structure when compared to the vehicle regulator, which proves that the presence of TiO_2 nanoparticles did not reduce cell viability [1, 9].

The present observations align with earlier reports demonstrating that PLA-based TiO_2 nanocomposites exhibit high biocompatibility along with added functionalities, including improved antimicrobial activity [7,28]. Overall, the evidence of low percentages of inhibition and preserved cellular morphology prove that PLA/TiO_2 nanocomposites films are safe and can be used where direct or indirect contact with biological systems is anticipated.

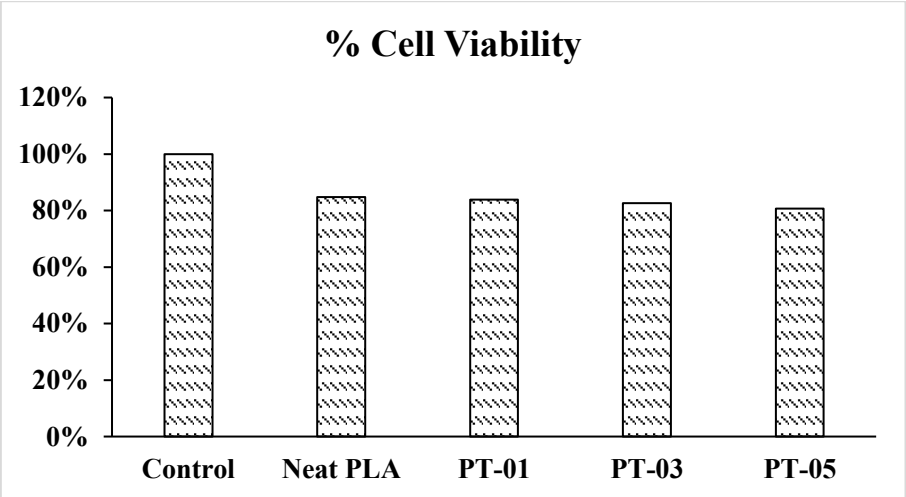
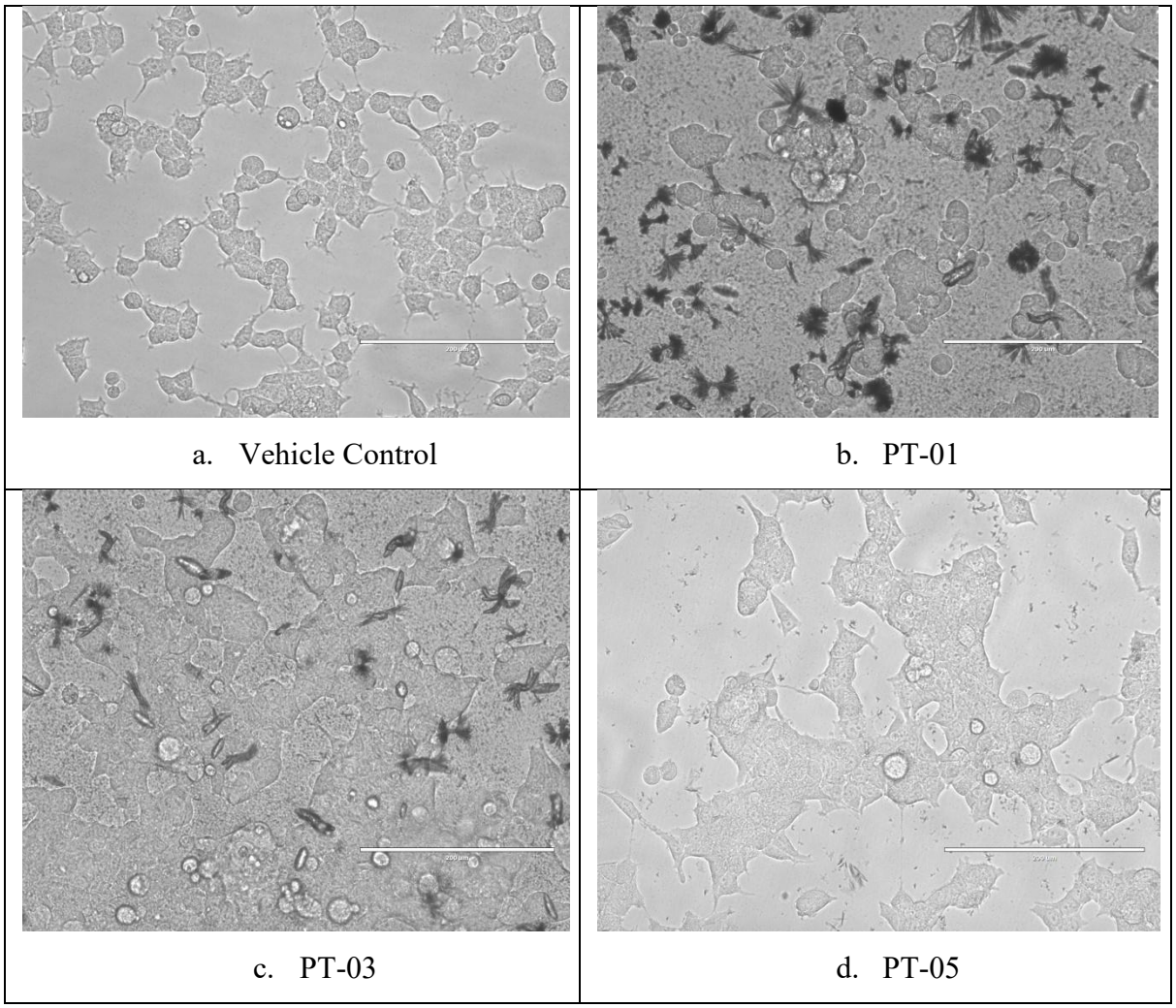


Figure_12 Cell viability percentage of PLA/TiO_2 nanocomposite films based on cytotoxicity study



a. Vehicle Control

b. PT-01

c. PT-03

d. PT-05

Figure_13 Microscopic cell morphology 24 hours following treatment with (a) vehicle control, (b) PT-01 (1 wt% TiO_2), (c) PT-03 (3 wt% TiO_2) and (d) PT-05 (5 wt % TiO_2) nanocomposite films.

Conclusion

In this study, PLA/TiO_2 nano composite films were successfully developed using the ultrasonication assisted solvent casting method. The structural analysis through FTIR and XRD confirmed strong interactions between PLA and TiO_2, such as hydrogen bonding and coordination effects, which enhanced the films' crystallinity and overall structural integrity. SEM observations showed that TiO_2 dispersed well at lower concentrations, while higher loading led to slight agglomeration, influencing the material's morphology.

The incorporation of TiO_2 significantly enhanced the structural properties of PLA films, increasing tensile strength and stiffness, though flexibility decreased as expected due to the

rigid nature of nano particles. Among all formulations, the 3 wt% TiO_2 composition (PT-03) offered the best balance of strength, stiffness, and flexibility. Barrier performance revealed that TiO_2 effectively reduced water vapor permeability and solubility by creating a more complex path for moisture, thereby enhancing water resistance. Thermal analysis further demonstrated that TiO_2 acted as a nucleating agent, improving thermal stability and crystallinity without altering the glass transition temperature.

Higher TiO2 content significantly hindered the growth of E. coli and S. aureus bacteria. Cytotoxicity tests confirmed the films' biocompatibility, thus can be used for food packaging applications.

Overall, TiO_2 nanoparticles proved to be multi-functional fillers, enhancing mechanical, thermal, barrier, and antibacterial properties of PLA films. The 3 wt% TiO_2 formulation emerged as the most effective, combining superior performance with processability, and indicating a strong potential for Eco-friendly, active packaging solutions.

References

1. Khalil, A.M., El-Sayed, S.M. & Youssef, A.M. Valorization of polylactic acid bionanocomposites enriched with CuO-TiO_2 for packaging applications. Biomass Conv. Bioref. 2025; 15, 3485–3494.
2. Triamnak, N., Suttiruengwong, S., Vittayakorn, N., Girdthep, S., &Khankrua, R., The properties investigations of PLA/TiO_2 and PLA/doped-TiO_2 composites films. Polymer-Plastics Technology and Materials. 2023; 62(12), 1576–1586.
3. Asim Z, Shamsi IRA, Wahaj M, Raza A, AbulHasan S, Siddiqui SA, Aladresi A, Sorooshian S, SengTeck T. Significance of Sustainable Packaging: A Case-Study from a Supply Chain Perspective. Applied System Innovation. 2022; 5(6):117.
4. Ibrahim ID, Hamam Y, Sadiku ER, Ndambuki JM, Kupolati WK, Jamiru T, Eze AA, Snyman J. Need for Sustainable Packaging: An Overview. Polymers (Basel). 2022 Oct 20;14(20):4430.
5. Segura González, E.A.; Olmos, D.; Lorente, M.Á.; Vélaz, I.; González-Benito, J. Preparation and Characterization of Polymer Composite Materials Based on PLA/TiO_2 for Antibacterial Packaging. Polymers. 2018; 10, 1365.
6. Yakdoumi, Fatima Zohra and Hadj-Hamou, AssiaSiham. "Effectiveness assessment of TiO_2-Al_2O_3 nano-mixture as a filler material for improvement of packaging performance of PLA nanocomposite films" Journal of Polymer Engineering. 2020; 40: (10): 848-858.
7. Rajendran DS, Venkataraman S, Jha SK, Chakrabarty D, Kumar VV. A review on bio-based polymer polylactic acid potential on sustainable food packaging. Food SciBiotechnol. 2024 Mar 12;33(8):1759-1788.
8. Wu, Y.; Gao, X.; Wu, J.; Zhou, T.; Nguyen, T.T.; Wang, Y. Biodegradable Polylactic Acid and Its Composites: Characteristics, Processing, and Sustainable Applications in Sports. Polymers. 2023; 15, 3096.
9. Li, J.; Zhang, D.; Hou, C. Application of Nano-Titanium Dioxide in Food Antibacterial Packaging Materials. Bioengineering. 2025; 12, 19.
10. Nosrati H, Heydari M. Titanium dioxide nanoparticles: a promising candidate for wound healing applications. Burns Trauma. 2025; 3;13:tkae069.
11. Feng, S.; Zhang, F.; Ahmed, S.; Liu, Y. Physico-Mechanical and Antibacterial Properties of PLA/TiO2 Composite Materials Synthesized via Electrospinning and Solution Casting Processes. Coatings 2019, 9, 525.

12. Escorcia-Díaz D, García-Mora S, Rendón-Castrillón L, Ramírez-Carmona M, Ocampo-López C. Advancements in Nanoparticle Deposition Techniques for Diverse Substrates: A Review. Nanomaterials. 2023; 13(18):2586.
13. Bergaliyeva S, Sales DL, Jiménez Cabello JM, Burgos Pintos P, Fernández Delgado N, MarzoGago P, Zammit A, Molina SI. Thermal and Mechanical Properties of Reprocessed Polylactide/Titanium Dioxide Nanocomposites for Material Extrusion Additive Manufacturing. Polymers (Basel). 2023; 18;15(16):3458.
14. Kaseem, M.; Hamad, K.; Ur Rehman, Z. Review of Recent Advances in Polylactic Acid/TiO2 Composites. Materials 2019, 12, 3659.
15. GiadaBelletti, Sara Buoso, Lucia Ricci, Alejandro Guillem, Alejandro Aragón Gutiérrez, Olga Bortolini, Monica Bertoldo, Preparations of Poly(lactic acid) Dispersions in Water for Coating Applications, Polymers. 2021; 13(16):2767.
16. R K Gond& M K Gupta, Preparation of PLA based biodegradable nanofibre films and their characterization, Indian Journal of Fibre & Textile Research. 2021; 46, 9-14.
17. Kosowska, K., & Szatkowski, P. (2020). Influence of ZnO, SiO_2 and TiO_2 on the aging process of PLA fibers produced by electrospinning method. Journal of Thermal Analysis and Calorimetry, 140, 1769–1778. https://doi.org/10.1007/s10973-019-08890-6
18. OrawanWiranwetchayan, SurinPromnopas, TitipunThongtem, ArnonChaipanich, SomchaiThongtem, Effect of alcohol solvents on TiO 2 films prepared by sol–gel method, Surface and Coatings Technology. 2017 326(2).
19. Dejene BK, Gudayu AD. Achieving performance and functionality in PLA-based packaging: Insights from hybrid composites with false banana (Enset) fiber and ZnO nanoparticles. *Journal of Thermoplastic Composite Materials*. 2024;38(6):2138-2168. doi:10.1177/08927057241288125
20. Buzarovska, A. (2013). PLA Nanocomposites with Functionalized TiO_2 Nanoparticles. *Polymer-Plastics Technology and Engineering*, *52*(3), 280–286. https://doi.org/10.1080/03602559.2012.751411
21. Li, S., Chen, G., Qiang, S., Yin, Z., Zhang, Z., & Chen, Y. (2020). Synthesis and evaluation of highly dispersible and efficient photocatalytic TiO2/poly(lactic acid) nanocomposite films via sol–gel and casting processes. International Journal of Food Microbiology, 335, 108763. https://doi.org/10.1016/j.ijfoodmicro.2020.10

22. Grząbka-Zasadzińska A, Piątek A, Klapiszewski Ł, Borysiak S. Structure and Properties of Polylactide Composites with TiO2-Lignin Hybrid Fillers. Int J Mol Sci. 2024; 16;25(8):4398.
23. Ana Antunes, Anton Popelka, Omar Aljarod, Mohammad K. Hassan, AdriaanStephanusLuyt, Effects of Rutile–TiO2 Nanoparticles on Accelerated Weathering Degradation of Poly(Lactic Acid), Polymers. 2020; 12(5):1096.
24. ASTM International. ASTM E8/E8M-16a: Standard Test Methods for Tension Testing of Metallic Materials. ASTM International, 2018.
25. Fatahi H, Claverie J, Poncet S. Thermal Characterization of Phase Change Materials by Differential Scanning Calorimetry: A Review. Applied Sciences. 2022; 12(23):12019.
26. Charles AL, Motsa N, Abdillah AA. A Comprehensive Characterization of Biodegradable Edible Films Based on Potato Peel Starch Plasticized with Glycerol. Polymers (Basel). 2022 Aug 25;14(17):3462.
27. Olaoye TS, Dewsbury M, Künzel H. Laboratory Measurement and Boundary Conditions for the Water Vapour Resistivity Properties of Typical Australian Impermeable and Smart Pliable Membranes. Buildings. 2021; 11(11):509.
28. Jin TZ, Fan X, Mukhopadhyay S. Antimicrobial effects of pulsed light activated TiO2-Polylactic acid film. Heliyon. 2024 Oct 2;10(20):e38891.
29. Khashan KS, Sulaiman GM, Abdulameer FA, Albukhaty S, Ibrahem MA, Al-Muhimeed T, AlObaid AA. Antibacterial Activity of TiO2 Nanoparticles Prepared by One-Step Laser Ablation in Liquid. Applied Sciences. 2021; 11(10):4623.
30. Chi H, Li W, Fan C, Zhang C, Li L, Qin Y, Yuan M. Effect of High Pressure Treatment on Poly(lactic acid)/Nano–TiO_2 Composite Films. Molecules. 2018 Oct 12;23(10):2621.
31. Tang, Z., Fan, F., Fan, C., Jiang, K., & Qin, Y. (2020). The performance changes and migration behaviour of PLA/nano-TiO_2 composite film by high-pressure treatment in ethanol solution. Polymers, 12(2), 471. https://doi.org/10.3390/polym12020471
32. Wang, Y., Wu, X., Guo, L., Li, Q., & Wang, S., Improvement of water retention properties of annealed PLA/TiO2 composite films used for concrete curing. Materials Today Sustainability,2023, 22, 100401.
33. Tang Z, Fan F, Chu Z, Fan C, Qin Y. Barrier Properties and Characterizations of Poly(lactic Acid)/ZnONanocomposites. Molecules. 2020 Mar 13;25(6):1310.

34. Rhim, Jong-Whan, Seok-In Hong, and Chang Sik Ha., “Tensile, Water Vapor Barrier and Antimicrobial Properties of PLA/Nanoclay Composite Films.” LWT – Food Science and Technology, 2009, 42(2):612–17.
35. J Alberton *et al* 2014 *IOP Conf. Ser.: Mater. Sci. Eng.* **64** 012010
36. Jiang, Ling, Ying Li, Jianhua Liu, and Xiangyu Yang, "Effects of Rutile–TiO_2 Nanoparticles on Accelerated Weathering Degradation of Poly(Lactic Acid)." Polymers, 2020, 12(6):1391.
37. Södergård, A., &Stolt, M., Properties of lactic acid based polymers and their correlation with composition. Prog. Polym. Sci.,2002, 27(6), 1123–1163.
38. Yakdoumi, H., &Hadj-Hamou, A. S. Effect of TiO_2–Al_2O_3 nanoparticles on the thermal and optical properties of PLA films. J. Polym. Environ.,2020, 28, 2942–2953.
39. Li, S., et al. Preparation of PLA/TiO_2 nanocomposite films by sol-gel method: Structure, thermal stability, and antibacterial activity. Food Hydrocolloids, 2020, 106, 105919.
40. Farhoodi, M., et al. Influence of TiO_2 nanoparticle loading on the crystallinity and thermal behavior of PLA composites. J. Appl. Polym. Sci.,2020, 137(44), 49234.
41. Deghiche, A., et al., Functionalized TiO_2 nanoparticles as nucleating agents in PLA: Effect on crystallization and thermal stability. Polymers, 2021, 13(2), 214.
42. Murariu, M., & Dubois, P, . PLA composites and nanocomposites: Emerging trends and challenges. Mater. Sci. Eng. R, 2021, 145, 100608.
43. Li, X., et al., “Enhanced Antibacterial Properties of PLA/TiO_2 Films via ROS Mechanisms.” Journal of Applied Polymer Science, 2022, 139(12): e51692.
44. Rhim, J.W., et al., “Active Packaging Applications of PLA-Based Nanocomposites Containing Metal Oxide Nanoparticles.” Food Hydrocolloids, 2021, 113:106556.
45. Armentano, I., et al., “PLA–Metal Oxide Nanocomposites for Active Food Packaging.” Progress in Polymer Science, 2020, 108:101275.
46. Kumar, S., et al., “Photocatalytic and Antimicrobial Efficacy of TiO_2 Incorporated Biopolymer Films.” ACS Omega, 2023, 8(5): 4512–4522.
47. ASTM International. (2005). *ASTM E96-05: Standard Test Methods for Water Vapor Transmission of Materials*. West Conshohocken, PA.
48. ISO. (2009). *ISO 10993-5:2009 — Biological evaluation of medical devices — Part 5: Tests for in vitro cytotoxicity*. International Organization for Standardization.
49. ASTM International. (2018). *ASTM D882-18: Standard test method for tensile properties of thin plastic sheeting*. West Conshohocken, PA.